# Fault Detection for Precision Mechatronics
## Online Estimation of Mechanical Resonances

Classens, Koen; Mostard, Mike; Van De Wijdeven, Jeroen; Maurice Heemels, W. P.M.H.; Oomen, Tom

**DOI**
10.1016/j.ifacol.2022.11.271

**Publication date**
2022

**Document Version**
Final published version

**Published in**
IFAC-PapersOnline

Available online at www.sciencedirect.com

ScienceDirect

IFAC Papers Online CONFERENCE PAPER ARCHIVE

IFAC PapersOnLine 55-37 (2022) 746–751

# Fault Detection for Precision Mechatronics: Online Estimation of Mechanical Resonances

**Koen Classens** [*,****] **Mike Mostard** [*]
**Jeroen van de Wijdeven** [**] **W.P.M.H. (Maurice) Heemels** [*]
**Tom Oomen** [*,***]

[*] *Department of Mechanical Engineering, Eindhoven University of Technology, Eindhoven, The Netherlands*
[**] *ASML, Veldhoven, The Netherlands*
[***] *Faculty of 3mE, Delft University of Technology, Delft, The Netherlands*
[****] *(e-mail: k.h.j.classens@tue.nl)*

**Abstract:** The condition of mechatronic production equipment slowly deteriorates over time, increasing the risk of failure and associated unscheduled downtime. A key indicator for an increased risk for failures is the shifting of resonances. The aim of this paper is to track the shifting resonances of the equipment online and during normal operation. This paper contributes to real-time parametric fault diagnosis by applying and comparing parameter estimators in this new context, highly relevant for next-generation mechatronic systems. The proposed fault diagnosis systems consist of recursive least squares algorithms and the effectiveness is illustrated on an overactuated and oversensed flexible beam setup, allowing to artificially manipulate its effective resonances in a controlled manner.



*Keywords:* Fault Diagnosis, Fault Detection, Fault Isolation, Fault Estimation, Parametric Fault, Multiplicative Fault, Predictive Maintenance, Mechatronic System

## 1. INTRODUCTION

Next-generation mechatronic production systems are becoming increasingly more demanding in terms of performance and as a result, more complex. Despite excellent system design and major developments in control theory, the condition of these systems still deteriorates over time, making maintenance unavoidable. Due to the high cost associated with downtime, the high-tech production industry is shifting from traditional maintenance towards predictive strategies, see Classens et al. (2021b) for details. To this end, real-time fault detection and isolation (FDI) is highly important for complex closed-loop controlled systems as it serves as a foundation for effective, targeted, and optimal scheduling of maintenance.

Over the past decades, real-time FDI has proven to be crucial. Particularly, in safety critical domains, such as the process industry, automotive applications, and the aerospace industry. Motivated by FDI problems in these domains, numerous surveys have appeared which illustrate successful application, e.g., Gertler (1991), Isermann (2005), Gao et al. (2015), and Venkatasubramanian et al. (2003). In contrast, real-time diagnosis in the high-precision mechatronics industry has not matured yet. In particular, fault diagnosis during normal operation, i.e., online and without dedicated experiments.

Faults are typically split into two broad categories: additive, such as sensor drift, and multiplicative, such as resonance characteristics (system properties), see, e.g., Isermann (2005). A method to detect additive faults is using residual generators. This method has been applied in the context of mechatronic systems, see Classens et al. (2021a). For multiplicative faults, other approaches are more suitable, e.g., originating from the domain of system identification such as the recursive least squares (RLS) algorithms, see Ljung (1987); Söderström and Stoica (2001). These methods are particularly tailored to dedicated persistently exciting inputs. In contrast, solely data from normal operation may be used. For that reason, additional practical aspects need to be addressed in order to achieve successful implementation. Shifting resonances are considered multiplicative faults. They are extremely important as multiplicative faults affect stability margins and closed-loop performance. Namely, the controller is typically based on the response of the fault-free system and dedicated controller components, such as notch filters, may even become harmful in the case of a shifting resonance.

Although important progress has been made for fault detection for complex engineered systems, at present accurate FDI of parametric faults and its effective application to mechatronic systems during regular operation has received little attention. The aim of this paper is to contribute to illustrate this potential. To this end, the contribution of this paper is threefold: 1) Illustrate effective real-time resonance tracking for mechatronic systems, 2)

⋆ This work is supported by Topconsortia voor Kennis en Innovatie (TKI), and is supported by ASML Research, Veldhoven, The Netherlands.


10.1016/j.ifacol.2022.11.271

Develop a mechatronic system to manipulate resonances in a controlled fashion, 3) Address the practical aspects essential for application.

This paper is organized as follows. The paper proceeds with the problem formulation in Section 2. Subsequently, in Section 3 the implemented recursive parameter estimator algorithms are introduced, and aspects regarding implementation are described in Section 4. An experimental case study, presented in Section 5, illustrates the effectiveness of the proposed approach and finally, a conclusion is given in Section 6.

## 2. PROBLEM FORMULATION

Consider the generic continuous-time (CT) single-input single-output (SISO) system description, $P : u \mapsto y$,

$$P(s) = \frac{a_0 + a_1 s + \ldots + a_{m-1} s^{m-1}}{1 + b_1 s + \ldots + b_n s^n}, \tag{1}$$

where $a_i$ denote the numerator coefficients, and $b_i$ denote the denominator coefficients. In particular, lightly damped motion systems can be described in an equivalent modal representation, $P_m : u \mapsto y$, as

$$P_m(s) = \sum_{i=1}^{n_{rb}} \frac{v_i w_i^\top}{s^2} + \sum_{i=n_{rb}+1}^{n_s} \frac{v_i w_i^\top}{s^2 + 2\zeta_i \omega_i s + \omega_i^2}, \tag{2}$$

see, e.g., Gawronski (2004), Preumont (2018). The number of rigid body modes is denoted by $n_{rb}$, and the total number of modes is denoted by $n_s$. The mode shapes are defined by $v_i$ and $w_i$, whereas $\zeta_i, \omega_i \in \mathbb{R}_+$ represent the relative damping and natural frequencies of the flexible modes.

*Remark 1.* Note that in case the system is suspended, e.g., by flexures, $n_{rb} = 0$.

*Remark 2.* Given a complex pole pair of a CT dynamical system, $s_i$, its corresponding natural frequency $\omega_i = |s_i|$ and its corresponding damping ratio $\zeta_i = -\cos(\angle s_i)$.

Mechatronic systems typically operate in closed-loop, see Fig. 1. The closed-loop controlled system, subjected to multiplicative faults, is augmented with the fault estimator $E$. The main objective is to design $E$ in order to estimate the moving resonance parameters, $\zeta_i$ and $\omega_i$, over time using real-time operational data $u$ and $y$.

*Remark 3.* A typical task could be following a higher order setpoint $r$ or a regulator problem ($r = 0$).

*Remark 4.* In this paper, the main focus lies on SISO systems, i.e., $u \in \mathbb{R}$, $y \in \mathbb{R}$, $v_i \in \mathbb{R}$, and $w_i \in \mathbb{R}$. The approach can be extended to multi-input multi-output (MIMO) systems, where $u \in \mathbb{R}^{n_u}$, $y \in \mathbb{R}^{n_y}$, $v_i \in \mathbb{R}^{n_y}$, and $w_i \in \mathbb{R}^{n_u}$.

## 3. PARAMETRIC FAULT DIAGNOSIS SOLUTION

Consider (1), with differential equation

$$y + b_1 \dot{y} + \ldots + b_n y^{(n)} = n_0 u + n_1 \dot{u} + \ldots + n_{m-1} u^{(m-1)}, \tag{3}$$

where $^{(n)}$ and $^{(m)}$ denote higher-order derivatives. At time-instance $k$, this relation can be written as

$$y(k) = \phi^\top(k)\theta, \tag{4}$$

where the output $y(k) \in \mathbb{R}^{n_y}$, the regressor matrix

$$\phi(k) = \left[-\dot{y}(k) \ \ldots \ -y^{(n)}(k) \ u(k) \ \dot{u}(k) \ \ldots \ u^{(m-1)}(k)\right]^\top \in \mathbb{R}^{n_\theta \times n_y},$$

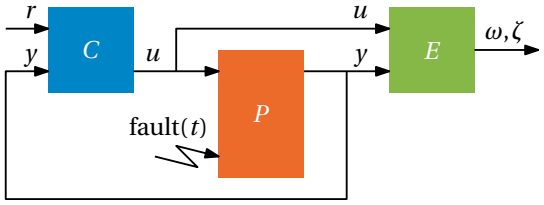


Fig. 1. Overview of the closed-loop control system and the fault diagnosis system. The controller $C$ (■), the plant $P$ (■), and the parameter estimator $E$ (■) are highlighted. The plant is subjected to faults and the estimator processes the control input $u$ and output $y$, giving information about natural frequencies $\omega$ and the corresponding relative dampings $\zeta$.

and the parameter vector

$$\theta = \left[-b_1 \ \ldots \ -b_n \ n_0 \ n_1 \ \ldots \ n_{m-1}\right]^\top \in \mathbb{R}^{n_\theta}.$$

The regressor contains measured signals or estimates based on the measured signals. The regressor couples the to-be estimated parameters $\theta$ to the measured output $y(k)$.

A recursive least squares (RLS) solution is presented which in addition to the parameter estimate generates information about the uncertainty (variance) of the estimation, see, e.g., Ljung (1987) for details. RLS algorithms aim to minimize the cost function

$$\mathcal{J}_{\text{RLS}}(k) = \frac{1}{2} \sum_{t=1}^{k} \left( e_{\text{opt}}^\top(\theta, k) \Lambda(k) e_{\text{opt}}(\theta, k) \right), \tag{5}$$

where $e_{\text{opt}}(\theta, k) = y(k) - \phi^\top(k)\theta$ is the prediction error and $\Lambda(k)$ a positive definite weighting matrix.

Note that in the previous, $\theta$ is not a function of the time instance $k$. In the case of shifting resonances, the parameters vary over time. To the end of estimating $\theta(k)$, the forgetting factor and the Kalman algorithm are used. Both algorithms are well-known in literature, are computationally cheap, and give the desired knowledge, making them attractive for online FDI.

### 3.1 Forgetting Factor RLS

The algorithm consists of three equations. Typically, $N_y \leq N_\theta$. In that case, the learning gain

$$L(k) = P(k-1)\phi(k) \left( \lambda(k)\Lambda(k) + \phi^\top(k) P(k-1) \phi(k) \right)^{-1}, \tag{6}$$

the parameter estimate

$$\theta(k) = \theta(k-1) + L(k) \left( y(k) - \phi^\top(k)\theta(k-1) \right), \tag{7}$$

and matrix

$$P(k) = \frac{1}{\lambda(k)} \left( P(k-1) - L(k)\phi^\top(k) P(k-1) \right), \tag{8}$$

with forgetting factor $\lambda(k) \in (0, 1]$. The matrix $P$ is a measure for the uncertainty of the estimate.

### 3.2 Kalman Estimator RLS

In the Kalman estimator, $\theta(k)$ is considered a Gaussian random vector with noise variance $R(k)$ and with measurements $y(k)$ containing noise with a covariance $Q(k)$. Similarly, the Kalman result consists of three equations. Namely, the learning gain

$$L(k) = P(k-1)\phi(k) \left( R(k) + \phi^\top(k) P(k-1) \phi(k) \right)^{-1}, \tag{9}$$

the parameter estimate

$$\theta(k) = \theta(k-1) + L(k)\left(y(k) - \phi^\top(k)\theta(k-1)\right), \quad (10)$$

and the covariance matrix

$$P(k) = P(k-1) + Q(k) - L(k)\phi^\top(k)P(k-1). \quad (11)$$

Next, a number of relevant aspects are discussed which enable successful implementation.

## 4. PRACTICAL ASPECTS FOR SUCCESSFUL IMPLEMENTATION

In this section, crucial aspects are addressed which are required for successful implementation of the presented estimator algorithms. First, it is described how to deal with the noisy continuous time signals and how to estimate derivatives. Subsequently downsampling is addressed. Then a strategy to enhance persistency of excitation is presented. Finally, the numerical stability of the resulting filters and closed-loop aspects are addressed.

### *4.1 Derivative Filter*

The underlying physical relations are described by CT differential equations instead of (approximate) discrete-time (DT) difference equations. The reason for this is that the CT relations directly contain physically interpretable parameters.

The use of CT differential equations, see Section 2, comes with the challenge that the regressor $\phi(k)$ likely contains CT derivatives of measured signals while the information about the system is available only at the sampled instances $k$. Hence, the derivatives must be approximated if not available directly from sensors. Solutions in literature include for instance the state variable filter, see Chamberlin (1980), and Peter and Isermann (1990). Next, an alternative pragmatic approach is presented, taking into account the following.

(1) The filter should be implementable, i.e., causal.
(2) The DT filter should approximate the CT filter up to a user-defined cut-off frequency.
(3) The filter should be of minimal order to reduce computational burden.
(4) The entries in the DT filter should be of numerically similar order.

Let $p$ denote the highest derivative in $\phi(k)$. Then define

$$Z = [1 \;\; s \;\; \ldots \;\; s^p]. \quad (12)$$

Subsequently, define a $p^{\text{th}}$ order lowpass filter $L$ with cutoff frequency $f_c$. Then multiplying $Z$ with the resulting $L$ gives $\hat{Z} = LZ$ which is a CT (strictly-)proper approximate of $Z$. Subsequently $\hat{Z}$ is discretized using Tustin discretization. The order of the resulting denominator polynomial is $p+1$, implying a minimal state-space dimension of $p$. The regressor and output signals are processed with the same approximate filter, respectively.

### *4.2 Downsampling*

Modern mechatronic systems operate at a very high sampling rate, typically higher than 1 kHz. The estimators do not have to run at these sampling rates and the data may be downsampled to decrease the computational burden of the estimator. Ultimately decreasing the sampling rate too far comes at the cost of a less accurate, and eventually diverging estimate with large variance.

### *4.3 Persistency of Excitation - Enable Disable Strategy*

A system is persistently excited when the system generates data which contains sufficient amount of information to extract the desired system properties. See Ljung (1987) for a formal definition.

Theoretically, it is straightforward to derive an expression for $y(k) = \phi^\top(k)\theta$, and the signals may seem independent. Consequently, a unique solution for $\theta$ is available. In an application, however, certain signals may not be excited sufficiently or sufficiently fast. This results in non-unique parameter estimates and a possibly large variance.

A strategy to overcome unsatisfactory results due to low excitation is to only enable the estimators during the time intervals of sufficient excitation of the regressor signals. There are multiple options for this enable/disable strategy.

(1) The enable signal can be a function of the setpoint and its derivatives. This is computationally cheap as all signals are predictable and available prior to operation.
(2) The enable signal can be a function of measured signals, such as actuator input, the output or its filtered derivatives.
(3) The enable signal can be a function of the combination of both setpoint and measured signals.

*Remark 5.* While disabling the algorithm, it is suggested to hold the last estimate of the parameters $\theta$ and corresponding covariance until the estimator is re-enabled.

### *4.4 Numerical Stability RLS Filters*

Despite the algorithms in Section 3 being correct, during implementation Ljung (1987) proposes alternatives for the forgetting factor and Kalman variants of the RLS algorithm which are more numerically sound. The alternative solves problematic round-off errors in $P(k)$ which can make this matrix indefinite over time. The solution is based on the fact that $P(k)$ can be decomposed by $Q(k)Q^\top(k)$. By recursively computing this, the corresponding $P(k)$ is forced to be positive-definite.

### *4.5 Closed-loop Aspects*

In practice, the output $y$ is perturbed by noise $v$. The proposed approaches do not take into account the effect of the presence of the controller $C$. Due to the controller in closed-loop systems, the input $u$ is a function of the output $y$ and as a result correlated with the noise $v$. A consequence of the correlation between $u$ and $v$ is that a (slightly) biased estimate is obtained.

*Remark 6.* If the correlation between noise $v$ and control input $u$ is low, the consequences are limited, e.g., when relatively accurate sensors are used such that the signal to noise ratio at the input is high. Alternative solutions exist in case the correlation is high, see Söderström and Stoica (2001).

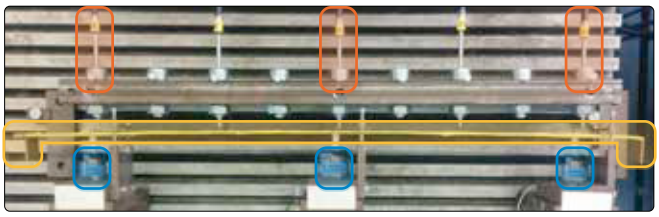

Fig. 2. Prototype experimental setup. The moving part, i.e., the flexible beam, is equipped with yellow tape and is outlined with (■). The beam is actuated by three voice coil actuators (■), and five fiber-optic displacement sensors, of which three are used (■). The steel beam is held up by four wire flexures from the table upwards, and one sideways on the left.

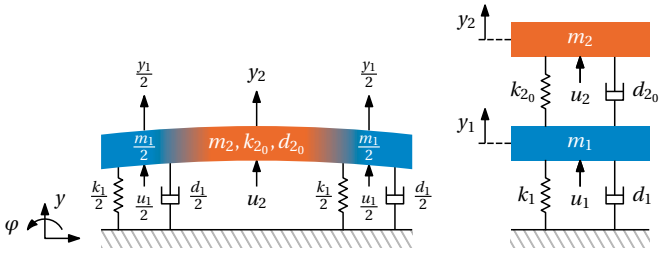


(a) Flexible beam system. (b) Equivalent system.

Fig. 3. Symmetric beam with inputs $u_1$, $u_2$, and outputs $y_1$, $y_2$. The system can be seen as a two mass-spring-damper system, where the first mass, $m_1$ (■), corresponds to the outer portion of the beam and the second mass, $m_2$ (■), corresponds to the inner mass.

*Remark 7.* For diagnostics purposes the true parameter values are of lesser importance as long as the estimates are approximately representative for the physics. It is more important that an estimation algorithm detects changes in the estimated parameter values as this is an indication that failure has occurred or is likely to occur in the future. For this reason, the resulting bias is less important w.r.t. for instance system identification for controller design.

## 5. EXPERIMENTAL VALIDATION

First the experimental flexible beam setup will be introduced, the transformation to an equivalent two degree of freedom mass-spring-damper system will be illustrated, and the artificial resonance manipulation will be described. Subsequently, the estimator results will be shown for multiple setpoints and multiple parametric fault trajectories. Here, the main focus lies on the application of the RLS algorithms.

### 5.1 Setup

A picture of the setup is shown in Fig. 2, where the main components are highlighted. The movable part of the system consists of a steel beam of 500 × 20 × 2 mm. Four degrees-of-freedom (DOFs) are fixed by means of wire flexures. Hence, two DOFs remain to be controlled, in addition to the flexible dynamical behavior. The remaining degrees of freedom are one translation, denoted by $y$, and the rotation $\varphi$. The setup is equipped with three current-driven voice-coil actuators, as well as contactless fiberoptic

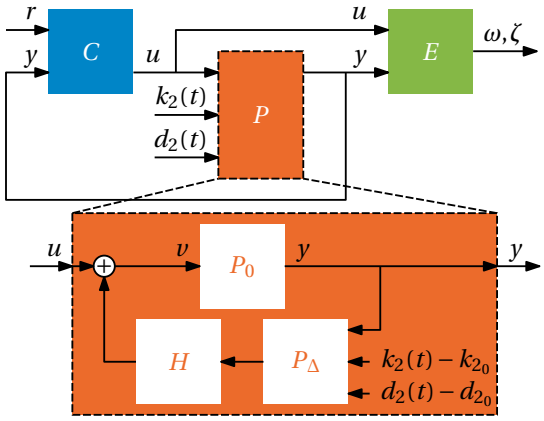


Fig. 4. Overview of the closed-loop control system and the fault diagnosis system. The controller $C$ (■), the plant $P$ (■), and the parameter estimator $E$ (■) are highlighted. The plant can be manipulated with $k_2(t)$ and $d_2(t)$. The additional control law $P_\Delta = (k_2(t) - k_{2_0}) + (d_2(t) - d_{2_0})\, s$, is a proportional derivative controller, where $k_{2_0}$ and $d_{2_0}$ denote the original stiffness and damping, respectively. Additionally, a delay compensator $H$ is incorporated in the internal feedback loop.

sensors with an accuracy of approximately 1 $\mu$m. The system is operating at a sampling frequency of 4096 Hz on a Raspberry Pi.

The flexible beam including the first internal resonance mode is schematically drawn in Fig. 3a. The rotational DOF is suppressed with a dedicated controller and due to symmetry, the system can be seen as the schematic drawing in Fig. 3b, with inputs $u_1$, $u_2$, and outputs $y_1$, $y_2$. The system has mechanical properties $m_1, m_2$, $k_1$, $k_{2_0}$, $d_1$, and $d_{2_0}$.

### 5.2 Resonance manipulation

To manipulate the effective resonances of the system, an input and output transformation is applied to isolate the flexible mode. An additional internal feedback loop is created for the flexible mode of the system with time-varying constants $k_2(t)$ and $d_2(t)$ which allow to vary the internal stiffness and damping of the beam over time, see Fig. 4. For details regarding the implementation, see Classens et al. (2021a).

The resulting system $P$ can be described by the state-space description

$$\dot{x} = Ax + Bu, \tag{13a}$$
$$y = Cx, \tag{13b}$$

with

$$A = \begin{bmatrix} 0 & 1 & 0 & 0 \\ -\frac{k_1+k_2(t)}{m_1} & -\frac{d_1+d_2(t)}{m_1} & \frac{k_2(t)}{m_1} & \frac{d_2(t)}{m_1} \\ 0 & 0 & 0 & 1 \\ \frac{k_2(t)}{m_2} & \frac{d_2(t)}{m_2} & -\frac{k_2(t)}{m_2} & -\frac{d_2(t)}{m_2} \end{bmatrix},$$

$$B = \begin{bmatrix} 0 \\ \frac{1}{m_1} \\ 0 \\ 0 \end{bmatrix}, \; C = [1\ 0\ 0\ 0]$$

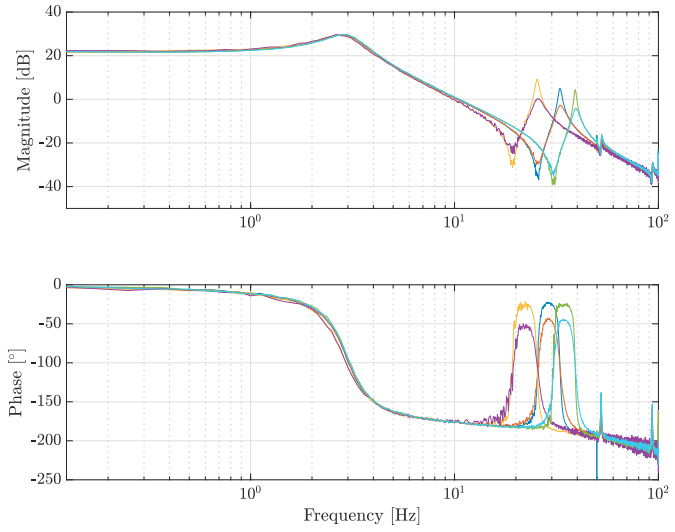


Fig. 5. Measured frequency response function where the second resonance is manipulated. The fault-free system (—) is indicated. Only increasing the damping $d_2(t)$ gives (—). Only increasing the stiffness $k_2(t)$ gives (—), whereas decreasing $k_2(t)$ gives (—). Combined shifts in $k_2(t)$ and $d_2(t)$ result in (—) and (—).

where the output $y := y_1 \in \mathbb{R}$, and the input $u := u_1 \in \mathbb{R}$. The transfer function matrix (TFM) of the system is equal to $P(s) = C(sI - A)^{-1}B$.

*Remark 8.* Note that the resulting transfer is now a function of $k_2(t)$ and $d_2(t)$ which can be manipulated over time to achieve time-varying resonance characteristics.

By manipulation of the stiffness $k_2$, the frozen frequency response function (FRF) shows, as expected, a shift in the second resonance of the system, see Fig. 5. Increasing the damping $d_2$ results in a higher damping as illustrated by the measured frozen FRFs.

Next, the parameters $k_2(t)$ and $d_2(t)$ are manipulated over time and the resonances are estimated online using the RLS algorithms presented in Section 3.

### 5.3 Fault Estimator

Given the model of the manipulated beam, i.e., (13) and its TFM $P(s)$ in the form (1), the to-be estimated vector $\theta$ can be derived which is equal to

$$\theta(t) = \begin{bmatrix} b_1(t) \\ b_2(t) \\ b_3(t) \\ b_4(t) \\ a_0 \\ a_1(t) \\ a_2(t) \end{bmatrix} = \begin{bmatrix} \frac{d_1}{k_1} + \frac{d_2(t)}{k_2(t)} \\ \frac{m_2}{k_2(t)} + \frac{m_1+m_2}{k_1} + \frac{d_1 d_2(t)}{k_1 k_2(t)} \\ \frac{d_1 m_2 + d_2(t) m_1 + d_2(t) m_2}{k_1 k_2(t)} \\ \frac{m_1 m_2}{k_1 k_2(t)} \\ \frac{1}{k_1} \\ \frac{d_2(t)}{k_1 k_2(t)} \\ \frac{m_2}{k_1 k_2(t)} \end{bmatrix}, \qquad (14)$$

with corresponding regressor

$$\phi^\top(k) = \begin{bmatrix} -\dot{y}(k) & \dots & -y^4(k) & u(k) & \dot{u}(k) & \ddot{u}(k) \end{bmatrix}. \qquad (15)$$

The system has two resonances. In the fault-free case, $\omega_1 \approx 3$ Hz, and $\omega_2 \approx 33$ Hz. Next, four experiments are performed and the RLS algorithms are compared in terms of their estimation of $\omega_i$ and $\zeta_i$.

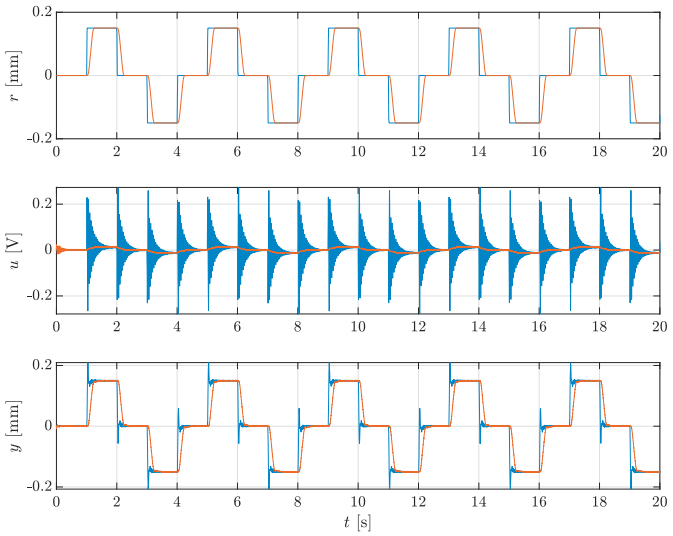


Fig. 6. The reference $r$ of experiment 1 and 3 (—) and the reference of experiment 2 and 4 (—). In addition, the corresponding input and output signals are depicted showing the time instances where the system is likely to be sufficiently excited or insufficiently excited.

For all experiments, the RLS with forgetting factor has $\lambda = 0.9992$ and $P(0) = 1 \cdot 10^{-2} I$. The Kalman covariance is set $P(0) = \text{diag}(2 \cdot 10^{-8}, 10^{-18}, 10^{-12}, 10^{-17}, 10^{-4}, 10^{-7}, 10^{-9})$.

The first experiment has a $0^{\text{th}}$ order reference, see Fig. 6 containing a snapshot of the fault-free situation. The fault consists of a step at $t = 90$ s in both $k_2$ and $d_2$, where the spring constant decreases and the damping constant increases. The first resonance remains fault-free. The second experiment has a $4^{\text{th}}$ order reference and the same fault. Both resulting estimates are depicted in Fig. 7.

The third experiment has a $0^{\text{th}}$ order reference and the fault is linearly increasing from $t = 60$ s to $t = 120$ s for $k_2$ and $d_2$. The fourth experiment has a $4^{\text{th}}$ order reference and the same fault. The resulting estimates are depicted in Fig. 8.

The natural resonance frequency as well as the damping constants are accurately estimated, especially with a $0^{\text{th}}$ order reference. With a $4^{\text{th}}$ order reference, the spread is larger as the regressors are excited to a lesser degree. Despite this, the shifting resonance is clearly detected. In addition, it can be concluded that the first damping constant is more difficult to detect.

Finally, a Nyquist diagram over time is shown of the estimated model during the experiment with $0^{\text{th}}$ order reference and linearly progressing fault, see Fig. 9. It can be observed that as the fault progressively becomes worse, stability margins drastically decrease, affecting closed-loop performance and increasing the risk of closed-loop instability.

## 6. CONCLUSION

This paper provides a model-based fault diagnosis framework to estimate parametric faults. In particular, shifting resonances in mechatronic systems. A system is designed

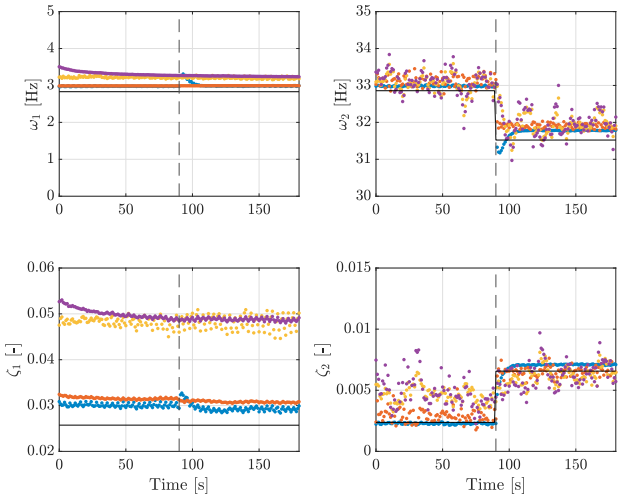


Fig. 7. Experiment with a step fault at $t = 90$ s in both $k_2$ and $d_2$. The expected parameters are indicated (—). The results of the first experiment, with $0^{\text{th}}$ order reference are depicted. The RLS with forgetting factor is shown in (•) and the Kalman RLS in (•). The estimates are both accurate and the shifting resonance is detected. Similarly, for the second experiment with $4^{\text{th}}$ order reference, the RLS with forgetting factor is shown in (•) and the Kalman RLS in (•). The shifting resonance is detected, despite a less exciting reference signal.

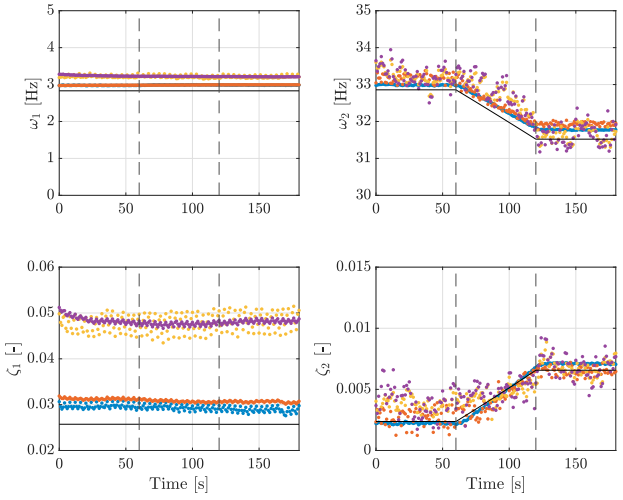


Fig. 8. Experiment with a linearly varying fault from $t = 60$ s until $t = 120$ s in both $k_2$ and $d_2$. The expected parameters are indicated (—). The results of the third experiment, with $0^{\text{th}}$ order reference are depicted. The RLS with forgetting factor is shown in (•) and the Kalman RLS in (•). The estimates are both accurate and the shifting resonance is detected. Similarly, for the fourth experiment with $4^{\text{th}}$ order reference, the RLS with forgetting factor is shown in (•) and the Kalman RLS in (•). The shifting resonance is detected, despite a less exciting reference signal.

to manipulate a single resonance peak in a controlled fashion. In addition, the crucial practical aspects are described. The proposed design shows real-time accurate estimation of the corresponding characteristics, namely the natural

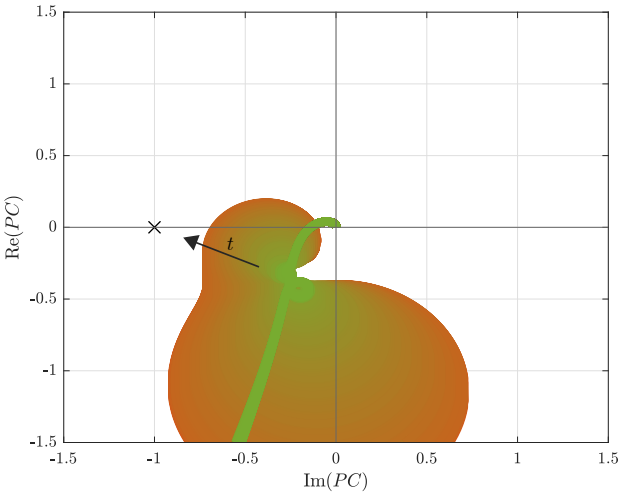


Fig. 9. Nyquist diagram over time of the second experiment. The open loop $PC$ at $t = 0$ s is indicated (—) and $PC$ at $t = 180$ s is indicated (—). The stability margins decrease as the fault increases.

frequencies and damping ratios. The approach is validated successfully on a closed-loop operated flexible beam system in real-time during normal operation. Even for smooth $4^{\text{th}}$-order setpoint trajectories, promising real-time diagnosis estimators are achieved. Hence, the potential for real-time resonance tracking has been shown, illustrating that this model-based fault diagnosis strategy can serve as an input for effective predictive maintenance for many closed-loop controlled mechatronic systems.

## REFERENCES

Chamberlin, H. (1980). *Musical Applications of Microprocessors*. Hayden Book Company.

Classens, K., Heemels, W.P.M.H., and Oomen, T. (2021a). A Closed-Loop Perspective on Fault Detection for Precision Motion Control: With Application to an Overactuated System. In *2021 IEEE International Conference on Mechatronics (ICM)*.

Classens, K., Heemels, W.P.M.H., and Oomen, T. (2021b). Digital Twins in Mechatronics: From Model-based Control to Predictive Maintenance. In *2021 IEEE International Conference on Digital Twins and Parallel Intelligence*.

Gao, Z., Cecati, C., and Ding, S.X. (2015). A Survey of Fault Diagnosis and Fault-Tolerant Techniques—Part I: Fault Diagnosis With Model-Based and Signal-Based Approaches. 62(6), 3757–3767.

Gawronski, W.K. (2004). *Advanced Structural Dynamics and Active Control of Structures*. Mechanical Engineering Series. Springer-Verlag.

Gertler, J. (1991). Analytical Redundancy Methods in Fault Detection and Isolation - Survey and Synthesis. 24(6), 9–21.

Isermann, R. (2005). Model-based fault-detection and diagnosis - status and applications. 29(1), 71–85.

Ljung, L. (1987). *System Identification - Theory for the User*. Prentice-Hall.

Peter, K. and Isermann, R. (1990). Parameter-Adaptive PID-Control Based on Continuous-Time Process Models. 23(1), 241–246.

Preumont, A. (2018). *Vibration Control of Active Structures*, volume 246 of *Solid Mechanics and Its Applications*. Springer International Publishing.

Söderström, T. and Stoica, P. (2001). *System Identification*. Prentice-Hall.

Venkatasubramanian, V., Rengaswamy, R., Yin, K., and Ka, S.N. (2003). A review of process fault detection and diagnosis Part I: Quantitative model-based methods. 19.